

The role of oxygen in hydrogen sensing by a platinum-gate silicon carbide gas sensor: An ultrahigh vacuum study

Yung Ho Kahng^{*}, Wei Lu, R. G. Tobin^{*}, Reza Loloee, and Ruby N. Ghosh

Citation: *Journal of Applied Physics* **105**, 064511 (2009); doi: 10.1063/1.3093688

View online: <http://dx.doi.org/10.1063/1.3093688>

View Table of Contents: <http://aip.scitation.org/toc/jap/105/6>

Published by the [American Institute of Physics](#)

AIP | Journal of
Applied Physics

Save your money for your research.
It's now **FREE** to publish with us -
no page, color or publication charges apply.

Publish your research in the
Journal of Applied Physics
to claim your place in applied
physics history.

The role of oxygen in hydrogen sensing by a platinum-gate silicon carbide gas sensor: An ultrahigh vacuum study

Yung Ho Kahng,^{1,a)} Wei Lu,¹ R. G. Tobin,^{1,b)} Reza Loloee,² and Ruby N. Ghosh²¹Department of Physics and Astronomy, Tufts University, Medford, Massachusetts 02155, USA²Department of Physics and Astronomy, Michigan State University, East Lansing, Michigan 48824, USA

(Received 6 November 2008; accepted 28 January 2009; published online 24 March 2009)

We report several experiments under ultrahigh vacuum conditions that elucidate the role of oxygen in the functioning of silicon carbide field-effect gas sensors with nonporous platinum gates. The devices studied are shown to be sensitive both to hydrogen and to propene. All of the results are consistent with oxygen acting through its surface reactions with hydrogen. Three specific aspects are highlighted: the need, under some conditions, for oxygen to reset the device to a fully hydrogen-depleted state; competition between hydrogen oxidation and hydrogen diffusion to metal/oxide interface sites, leading to steplike behavior as a function of the oxygen:hydrogen ratio (λ -sensing); and the removal of sulfur contamination by oxygen. © 2009 American Institute of Physics. [DOI: 10.1063/1.3093688]

I. INTRODUCTION

Metal-oxide-semiconductor devices based on silicon carbide, with gates made of catalytically active transition metals such as platinum and palladium, show great promise as sensors for hydrogen and other gases in harsh environments¹ involving high temperatures [up to 1000 °C (Refs. 2–4)] and corrosive gases.^{2,5,6} Figure 1 shows a schematic diagram of a typical device. Such devices have been successfully demonstrated for monitoring automotive exhaust,^{7,8} flue gases from power plants,^{9–11} and selective catalytic reduction in diesel engines.¹²

Our understanding of the sensing mechanism is based largely on the pioneering work of Lundström and co-workers,^{13–19} Kreisl *et al.*,^{20,21} and Salomonsson *et al.*²² on similar silicon-based devices. A series of careful studies in ultrahigh vacuum was instrumental in elucidating the key surface chemical processes involved.^{16–19} In the case of SiC devices, the investigation of fundamental mechanisms has been less extensive.^{23–25} Reference 26 presents a model of the hydrogen/oxygen response of these SiC sensors operating under atmospheric conditions at 700 K. There has been only one reported UHV study, focusing on the influence of sulfur.²⁷ We extend that UHV investigation with a series of observations centered on the role of oxygen, finding that oxidation of adsorbed hydrogen to form OH and water on the gate surface is the most important process.

Figure 1 also depicts schematically the major chemical reactions involving the gate. The key reactions necessary for hydrogen sensing are as follows:

- (1) Dissociative adsorption of hydrogen on the gate surface and its inverse, recombinative desorption,



Here V_s denotes a vacant adsorption site on the gate surface, and the notations g and a refer to gas phase and adsorbed species, respectively.

- (2) Diffusion of the H atoms through the gate metal between the gate surface and the metal/oxide interface, where they produce a dipole layer that shifts the capacitance-voltage (C - V) characteristic of the device toward a more negative bias,



where i denotes the metal/oxide interface. The sensor signal is obtained by monitoring the chemically induced shift in device potential, at constant capacitance, as a function of hydrogen concentration. Because hydrogen diffusion through the thin platinum layer is rapid at the sensor operating temperature,^{26,28} the concentrations of hydrogen on the gate surface and at the metal/oxide interface can be assumed to be in thermal equilibrium at all times.

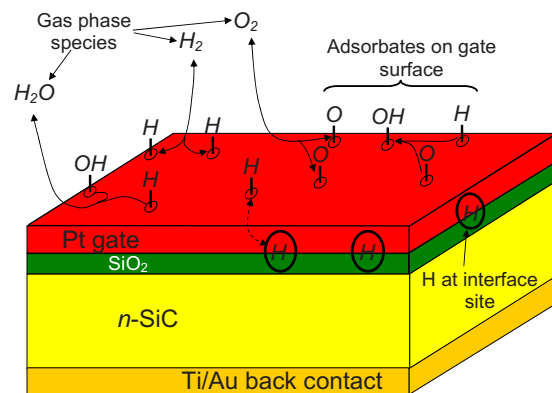


FIG. 1. (Color online) Schematic diagram of the device, showing the layered structure and the major surface reactions.

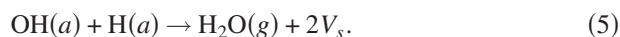
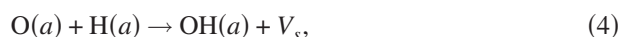
^{a)}Present address: Korea Research Institute of Standards and Science, Yuseong, Daejeon 305-340, Republic of Korea.

^{b)}Author to whom correspondence should be addressed. Electronic mail: roger.tobin@tufts.edu.

The detailed nature of the metal/oxide interface and of the hydrogen bonding sites is not fully understood. A detailed study of Si-based Pd-gate devices found evidence for sites on the oxide side of the interface,¹⁸ and a study of Pt-gate devices suggested that good gas sensitivity occurs only when the metal-oxide contact is poor.²⁹ Our SiC-based devices, however, operate at much higher temperatures, display different adsorption kinetics,¹¹ and exhibit both strong gas response and good film adhesion. In any case, for the present study the details of the interface are not important: all our analysis requires is that interface sites that give rise to the sensor response exist and that diffusion from the Pt surface to those sites be rapid.

Reference 26 reports experiments at atmospheric pressure and elevated temperatures (>700 K) in which hydrogen was found to have an additional effect through its passivation of electronic states at the SiO₂-SiC interface. This process was manifested through a slow and bias-dependent component of the sensor response and through a change in the shape of the *C-V* curve between hydrogen and oxygen ambients. The effect was minimized by choosing the bias point near midgap. Because of the choice of bias point and the lower operating temperature in the present work, we do not expect the role of hydrogen at the oxide-semiconductor interface to be significant.

When oxygen is present in the gas phase, it can also adsorb on the surface [for platinum gates, oxygen desorption becomes significant above about 450 °C (Ref. 30)] and can react with adsorbed hydrogen to form OH, which can then react to form water, which rapidly desorbs,



This simplified model assumes a single type of adsorption site for oxygen, hydrogen, and their reaction products and is broadly consistent with what is known about the adsorption and reaction of oxygen and hydrogen on Pt surfaces. A more detailed kinetic analysis for the rough surfaces of our gates would need to include the important role of steps and defects in promoting both dissociation and reaction.³¹

These reactions can affect the sensor signal indirectly in several ways: adsorbed oxygen can block surface adsorption sites, preventing hydrogen from sticking, and it can remove hydrogen from the surface through water formation and desorption. The effect is indirect because oxygen does not interact directly with hydrogen at the metal/oxide interface. But by lowering the concentration of hydrogen on the gate surface, it also reduces the concentration of interface hydrogen and thus the sensor signal. The influence of adsorbed oxygen on the sensor signal under atmospheric conditions has been discussed in Ref. 26.

If the gate metal is porous, additional effects involving the oxide-gas and oxide-gas-metal interfaces must be considered, such as hydrogen or oxygen spillover from the metal to the oxide.^{7,24} In the present studies, unlike those conducted

by other groups,^{9,11,12,24} the gates were continuous, nonporous gates in direct contact with the oxide,³² so these extra processes do not arise. In particular, direct adsorption of oxygen on the oxide surface, which has been proposed as an important mechanism for porous-gate devices,²⁴ is not significant for the sensors studied here. Instead the model given above, in which oxygen adsorbs and reacts only on the Pt surface and has only indirect effects on the sensor signal, is sufficient to explain the observed results.

II. EXPERIMENTAL PROCEDURES

With the exception of the measurements reported in Sec. III A, the experiments reported here were carried out on a single device, fabricated on an *n*-type 6H-SiC substrate (Cree, Inc.). The epitaxial layer was 3.6 μm thick with N dopant density of 2.1×10^{16} N/cm³. The SiO₂ layer was 39.5 nm thick and was grown by dry oxidation at 1150 °C followed by a 900 °C argon anneal and a 1175 °C NO anneal.³³ The catalytic gates were 100 nm thick platinum, grown by sputter deposition through a shadow mask at a sample temperature of 350 °C in 2.5 mTorr Ar. Fifty-two circular Pt gates were deposited on a 1 cm² chip, with nominal diameters of 200, 300, 500, and 1000 μm. The back side of the sample was metallized with 2 nm Ti followed by 100 nm Au. This deposition process yields continuous, nonporous gates in direct contact with the oxide.³² As a result our devices differ, particularly in their response to gases other than hydrogen, from those described by other groups that use multilayer or porous Pt gates. Further details of the sample preparation can be found in Refs. 27 and 34. After the gate deposition, the sample was mounted on an alumina header using silver paint (GC Electronics, Silver Print II), and 25 μm thick gold wire was wire bonded to selected gates and connected to gold pads on the header.

As has been observed previously,^{4,10,25} the as-fabricated device showed little or no sensitivity to hydrogen. The sample was therefore “activated” by alternating exposures of 1% O₂ in N₂ (5 min) and 10% H₂ in N₂ (3 min) for 7 h at a flow rate of 40 SCCM (SCCM denotes standard cubic centimeter per minute) while maintaining the device temperature at 610 °C (see Ref. 11 for experimental details). This procedure greatly enhances the performance of the sensor³⁵ through mechanisms that are not yet understood. One effect of the activation procedure is clearly a roughening of the Pt-gate surface that is visible both to the unaided eye and under the microscope.^{27,35,36} Despite these dramatic changes in appearance, the surface composition as revealed by Auger electron spectroscopy (AES) remains pure Pt, and x-ray diffraction measurements show that the bulk crystal structure remains that of elemental platinum. The changes in the gate during activation therefore appear to be purely morphological rather than changes in composition.

Following activation, the sample was mounted in an ion-pumped ultrahigh vacuum chamber with a base pressure of $\sim 2 \times 10^{-10}$ Torr and cleaned by standard surface science methods. Details of cleaning, temperature control, and gas dosing can be found in Ref. 27. Electrical measurements were made *in situ* using a 1 MHz capacitance bridge. For

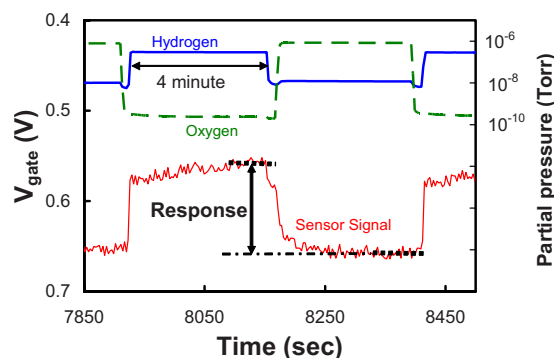


FIG. 2. (Color online) Example of a typical measurement of the sensor response to hydrogen in ultrahigh vacuum. H_2 (upper solid) and O_2 (dashed) partial pressures and sensor signal are plotted. The device was maintained at a constant capacitance of 450 pF by a feedback system and exposed alternately to hydrogen and oxygen; the gate voltage shift between the two conditions is taken to be the sensor response to the hydrogen pressure used. Partial pressures are indicated on the right axis, and the sensor signal is indicated on the left axis (note the inverted scale). The device temperature was 527 °C (800 K). From Kahng, Tobin, Loloee, and Ghosh, *J. Appl. Phys.* **102**, 064505 (2007). ©2007, American Institute of Physics.

sensor response measurements, a feedback system varied the gate bias to keep the device at a constant capacitance, which was selected near the midgap point for optimum performance.²⁶

Figure 2 illustrates one cycle of a typical sensor response measurement. The sample was maintained at a constant temperature of 527 °C (800 K) and biased at a fixed capacitance of 450 pF near the midgap point of the C - V curve. The graph shows the partial pressures of oxygen and hydrogen together with the gate voltage (note the inverted scale for the voltage) as a function of time. The sequence begins with the sample in an oxygen-rich environment to provide a hydrogen-depleted baseline. The oxygen flow is then stopped, and hydrogen is introduced to a specified partial pressure. The accumulation of hydrogen at the metal/oxide interface sites shifts the C - V curve to lower voltages, so to maintain a constant capacitance the bias voltage must be reduced. This bias shift is the sensor response. The hydrogen valve is then closed, oxygen is admitted to restore the hydrogen-depleted state, and the process is repeated.

Figure 3 shows a typical sequence of such measurement cycles, with varying hydrogen pressures, together with a plot of sensor response as a function of hydrogen pressure derived from the data. The device shows the Nernstian proportionality of sensor response to the logarithm of hydrogen pressure characteristic of electrochemical devices; for silicon-based devices, this proportionality has been demonstrated over nine orders of magnitude.¹⁶ Under UHV conditions, we consistently observed this logarithmic dependence of response on hydrogen pressure, but the slope (23 ± 3 mV/decade for the data shown) varied over the course of several months of study. In studies of similar devices under atmospheric conditions, the sensor response was much larger¹¹ and more closely proportional to the square root (rather than the logarithm) of the hydrogen concentration¹¹ and was far more stable over time.³² The variations in sensitivity under UHV conditions are not yet understood but may arise from changes in gate morphology.³⁵

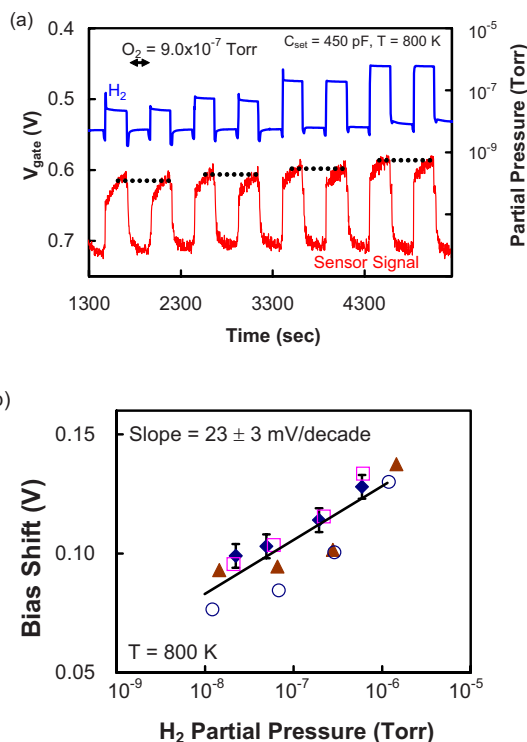


FIG. 3. (Color online) Signal and response to hydrogen for a clean sensor in UHV. (a) Gate voltage (sensor signal) at constant capacitance showing shifts in response to various partial pressures of hydrogen. Between hydrogen pulses, oxygen was admitted at a partial pressure of 9×10^{-7} Torr. The H_2 partial pressures used were 5.6×10^{-8} , 1.2×10^{-7} , 4.8×10^{-7} , and 1.5×10^{-6} Torr, with two pulses at each pressure. Dashed lines indicate the sensor responses. (b) Sensor response as a function of hydrogen partial pressure. The symbols indicate the results of four independent measurements; the error bars shown are typical of all four sets. The voltage shift is proportional to the logarithm of the hydrogen partial pressure, with a slope of 23 ± 3 mV/decade. From Kahng, Tobin, Loloee, and Ghosh, *J. Appl. Phys.* **102**, 064505 (2007). ©2007, American Institute of Physics.

The same essential mechanism allows the detection of any hydrogen-containing molecule that will dehydrogenate on the surface of the catalytic gate. Many hydrocarbons meet these criteria and can be detected,^{3,4,8,24,40} as can hydrogen sulfide.³⁷ Figure 4 shows the device response to propene (C_3H_6), a prototypical linear unsaturated hydrocarbon. A strong response is observed. Quantitative sensitivity measurements proved difficult, however, because we were unable to obtain an accurate calibration of the propene partial pressure and because of the long residence time of propene in the UHV chamber. Note the increase in sensor signal when the oxygen pressure is reduced at about 2500 s, even though no additional propene was admitted to the chamber. This increase is presumably a response to the high level of propene remaining in the chamber from the previous exposure.

III. RESULTS AND DISCUSSION

A. Possible role of oxygen in hydrogen depletion at low temperature

To be useful, a sensor's response should be reversible—when the stimulus is removed, the sensor signal should return to its baseline level. In the present context, reversibility requires that when the hydrogen level in the gas is reduced,

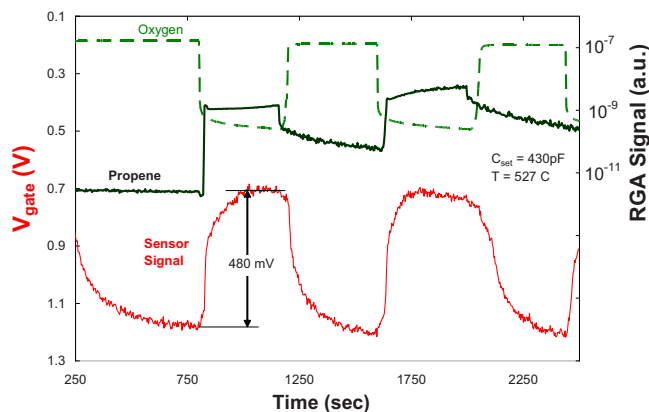


FIG. 4. (Color online) Sensor response to alternating pulses of propene (C_3H_6) and oxygen in ultrahigh vacuum. The sensor signal is indicated on the left axis (note the inverted scale). On the right axis are plotted raw RGA signals for the two gases, which are proportional to the partial pressure. The RGA sensitivity to propene is several hundred times lower than that to oxygen, so the relative partial pressure of propene was much higher than the graph suggests. The device temperature was $527\text{ }^\circ\text{C}$ (800 K).

the concentration of hydrogen bonded at the metal-oxide interface sites should also decrease, leading to a decrease in the bias voltage shift. In the absence of oxygen, this process must take place by diffusion of hydrogen atoms from interface to surface sites, followed by recombinative desorption of H_2 from the Pt surface [Eqs. (1) and (2)]. The rate of recombinative desorption will depend on the surface hydrogen concentration, the temperature, and the catalytic activity of the surface.

Figure 5 shows an experiment in which complete reversibility could not be achieved by hydrogen desorption alone but was accomplished by exposure of the device to oxygen. The experiment was carried out at a relatively low temperature of $327\text{ }^\circ\text{C}$ (600 K), 200 K lower than the other sensor measurements reported here, on a device that had not undergone “activation” outside the UHV chamber and therefore had a smoother gate presumably with a lower density of atomic defects and correspondingly lower catalytic activity

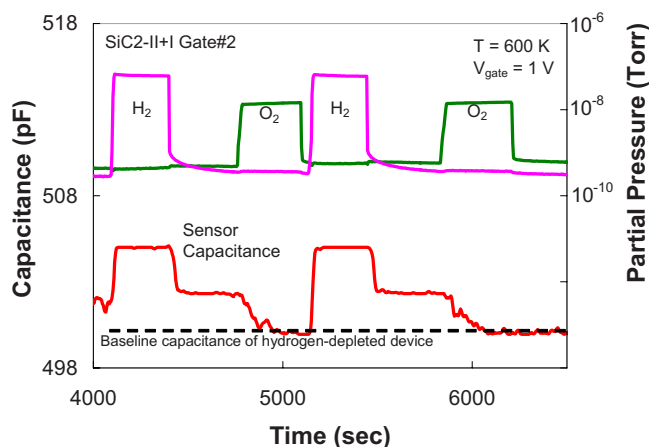


FIG. 5. (Color online) Effect of oxygen on sensor reversibility for a sensor with a nonactivated gate, operated at $327\text{ }^\circ\text{C}$ (600 K), 200 K lower than the other measurements reported. When the hydrogen pulse is ended, the capacitance does not return fully to the hydrogen-depleted baseline. For this device at this low temperature, a brief oxygen exposure is required for complete hydrogen depletion.

compared to those that were activated at atmospheric pressure.³⁵ In this case the device was held at fixed bias voltage, and the change in device capacitance in response to the gas exposures was monitored. The device was first exposed to a hydrogen pulse (6×10^{-8} Torr), resulting in a shift in the capacitance. When the hydrogen was shut off, the capacitance decreased due to the removal of hydrogen via recombinative desorption but then decreased further when the device was exposed to oxygen (1×10^{-8} Torr). The sequence was then repeated with the same results.

Evidently, for this device at this relatively low operating temperature, thermal desorption of hydrogen was insufficient to reset the device to its fully hydrogen-depleted baseline state, but that state could be easily achieved by a brief exposure to oxygen, presumably through hydroxyl and water formation followed by water desorption [Eqs. (4) and (5)]. Since both hydrogen desorption and water formation first require that hydrogen atoms migrate from the metal/oxide interface to the Pt surface, that migration step cannot be rate limiting. Recombinative hydrogen desorption, however, is second order in the surface hydrogen coverage since it requires the reaction of two surface-adsorbed hydrogen atoms. Therefore as the concentration of hydrogen in the device drops, the rate of hydrogen desorption decreases even faster. Hydroxyl and water formation, however, are first order in the hydrogen coverage, so they remain efficient channels for depleting the interface states even as the hydrogen concentration decreases.

These results are illustrative of the strong coupling between reactions on the gate surface and the occupation of the metal/oxide interface sites that provide the sensor signal. They also clearly demonstrate the role of oxygen in the removal of hydrogen from the device. Because of the low operating temperature and the use of a nonactivated gate, however, they may be of little direct relevance to practical devices. With higher temperatures and a more active gate surface, recombinative desorption of hydrogen, even without oxygen, may be sufficient to deplete the interface states.

B. λ -sensing behavior

Sensors that depend on the catalytic activity of a metal gate tend to exhibit nearly step-function responses to the inverse redox ratio λ , which is a measure of the ratio of oxidizing to reducing stream in the gas stream, defined so that $\lambda=1$ when the mixture is stoichiometric. Such behavior is seen, for example, in the zirconia-based oxygen sensors used in automotive exhaust systems,³⁸ and it has previously been observed for SiC field-effect sensors under atmospheric-pressure conditions.^{25,39–41} Qualitatively, it results from a kinetic phase transition between oxygen-dominated and hydrogen-dominated surface conditions.⁴²

Figure 6 shows a similar step response observed under UHV conditions. In these experiments, the sample was held at $527\text{ }^\circ\text{C}$ and exposed to a constant partial pressure of oxygen, either 2×10^{-7} or 4×10^{-7} Torr. Hydrogen pulses at various partial pressures, from 10^{-7} to 10^{-5} Torr, were admitted, with the oxygen partial pressure maintained at its

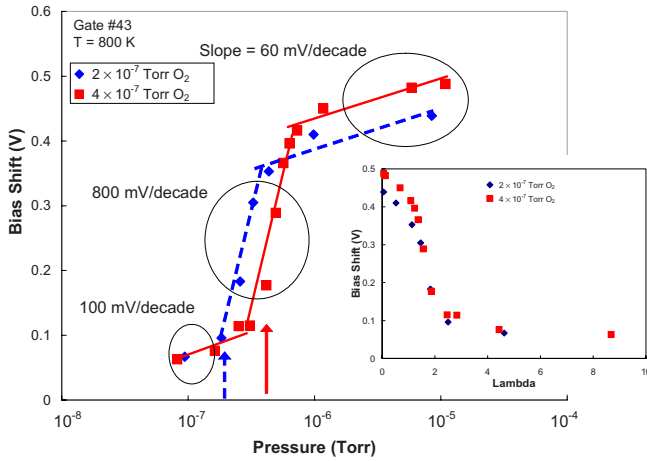


FIG. 6. (Color online) Sensor response as a function of hydrogen partial pressure, in the presence of a constant oxygen background, for two oxygen levels (indicated by the vertical arrows). Inset: The same data plotted as a function of the inverse redox ratio λ .

constant level. The sensor signal was taken to be the bias shift between the level in the oxygen background and the level during the hydrogen pulse.

When the hydrogen pressure is substantially lower than the oxygen pressure, the signal is very small because most of the hydrogen is immediately oxidized and removed, so that the hydrogen concentration on the gate surface, and therefore also at the metal/oxide interface sites, is low. When the hydrogen pressure is substantially higher than the oxygen pressure, the bias shift is much larger because not enough oxygen is available to react with the hydrogen and the response approaches that of a clean sensor without oxygen. Between these two limits is a narrow transition region where the sensor response is roughly ten times more sensitive to hydrogen pressure than in either limit. In this regime an increase in the flux of hydrogen molecules reaching the surface increases the surface hydrogen coverage (and therefore the sensor signal) both by increasing the rate of direct adsorption [Eq. (1)] and by reducing the concentration of surface oxygen and therefore the rate at which hydrogen is removed from the surface through water formation [Eqs. (4) and (5)].

The inset shows the same data plotted as a function of the inverse redox ratio λ ,

$$\lambda = \frac{2[\text{O}_2]}{[\text{H}_2]}, \quad (6)$$

where $[\text{O}_2]$ and $[\text{H}_2]$ represent the effective partial pressures of oxygen and hydrogen at the sample surface, as determined from residual gas analyzer (RGA) readings corrected for the doser enhancement (for oxygen) and RGA sensitivity. Strictly speaking, the denominator in Eq. (6) should be a weighted sum of the partial pressures of all the reducing gases present in the ambient.⁴⁰ During these measurements, the only reducing gas (other than hydrogen) with a detectable partial pressure was CO, and the partial pressures of CO were always at least two orders of magnitude below that of hydrogen and so could be neglected. Plotted in this way, the two sets of data are virtually indistinguishable and show a

transition centered on $\lambda_c \approx 1.5$, somewhat to the oxidizing side of stoichiometry.

Measurements on a different gate on the same chip taken several months later showed a smaller sensor response, but the shape of the λ -dependence was the same, with the same value of λ_c and width of the transition region. The consistency of the λ -dependence, even as other device properties change, probably reflects the fact that it is determined by the catalytic activity of the Pt surface and is insensitive to the internal properties of the metal-oxide-semiconductor structure.

The fact that the transition does not occur at $\lambda=1$ is not surprising. In a series of studies of the λ -sensing behavior of catalytic gate SiC field-effect sensors at atmospheric pressure, Lloyd Spetz and co-workers^{25,39,41} observed transition values λ_c from 1 to ~ 2.5 , depending on sensor temperature, gas flow rates, and exposed area of catalytic surface. Their analysis assumes the surface chemical model summarized in Sec. I, in which the only role of oxygen is as a surface reactant for hydroxyl and water formation. They distinguished three limiting regimes: injection limited, diffusion limited, and reaction limited, depending on the extent to which mass transport and reactions away from the sensor gate affect the composition of the gas impinging on the gate surface. The transition is expected to occur at the stoichiometric point $\lambda=1$ only in the injection-limited case.^{25,39}

Under UHV conditions, where the mean free path of a gas molecule is much greater than the chamber dimensions, the process is always “reaction limited,” and for low steady-state coverages (i.e., if the temperature is high enough that water formation reaction occurs rapidly) the transition value λ_c is given by the ratio of the rates at which the reactants arrive at and adsorb on the surface,³⁹

$$\lambda_c = \frac{v_{\text{H}_2} S_{\text{H}}}{v_{\text{O}_2} S_{\text{O}}} = \sqrt{\frac{m_{\text{O}_2} S_{\text{H}}}{m_{\text{H}_2} S_{\text{O}}}} = 4 \frac{S_{\text{H}}}{S_{\text{O}}}, \quad (7)$$

where v represents the average thermal velocity of each species, m is its molecular mass, and S is its sticking coefficient. Our observed value of λ_c thus suggests $S_{\text{H}}/S_{\text{O}} \approx 0.4$. This ratio is lower than one might expect (i.e., one might expect a *higher* value of λ_c , even further to the oxidizing side of stoichiometry). Sticking coefficients on Pt(111) at room temperature are approximately 0.05 for oxygen^{43,44} and 0.07–0.10 for hydrogen.^{45–47} Dissociative sticking probabilities, however, vary with sample temperature^{44,48} and are strongly enhanced by the presence of surface defects such as steps.^{43,45,46,48–50} As discussed in Sec. II, device activation roughens the gate surface and must therefore produce a high density of surface defects, but the detailed structure and its effect on the surface reactivity are unknown. A ratio $S_{\text{H}}/S_{\text{O}} \approx 0.4$ is therefore not unreasonable and is consistent with our model of the role of oxygen as a surface reactant.

Figure 7 shows a similar experiment with propene. The results are qualitatively similar. In this case the RGA sensitivity to propene is unknown, so an arbitrary sensitivity factor has been assumed to place the transition near $\lambda=1.5$. The shape of the curves and the fact that the transition occurs

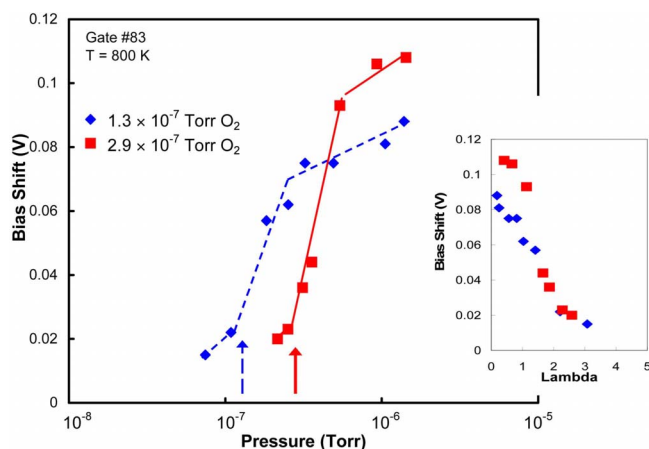


FIG. 7. (Color online) Sensor response as a function of approximate propene partial pressure, in the presence of a constant oxygen background, for two oxygen levels (indicated by the vertical arrows). Inset: The same data plotted as a function of the inverse redox ratio λ . Since the RGA sensitivity to propene is not known, the quantitative values of propene pressure and λ are arbitrary.

over the same λ range for both oxygen pressures are meaningful, but the numerical values of the propene pressure and λ values are not.

An interesting additional feature of the data, seen for both gates studied and for both hydrogen and propene, is that the sensor response under hydrogen-rich conditions is higher for higher oxygen background pressure. Since the response is measured as the difference in signal between the sensor in hydrogen and in the oxygen background, it is possible that a higher oxygen background more fully depletes the interface states of hydrogen, leading to a larger bias shift.

C. Removal of adsorbed sulfur with hydrogen and oxygen

A detailed study of the effects of sulfur on these devices has been published elsewhere.²⁷ Here we highlight results relating to the influence of oxygen. Since sulfur is a well-known poison for catalytic reactions on transition metal surfaces,^{51–55} it is not surprising that exposure to hydrogen sulfide under UHV conditions results in contamination of the gate surface and suppresses the device response. This contamination occurs even when oxygen or hydrogen is present in the gas phase at levels much higher than that of the sulfide.

Figure 8 shows the response of the device, at 527 °C, to alternating hydrogen and oxygen pulses before and immediately following a brief exposure to H_2S . Before the experiment AES showed that the gate surface was free of sulfur and other contaminants, and immediately after the H_2S dose showed a sulfur coverage of 0.38 ML (ML: 1 ML=1 S atom per surface Pt atom). The oxygen partial pressure was $\sim 10^{-10}$ Torr during the hydrogen pulses and $\sim 10^{-6}$ Torr between them.

For the first two oxygen/hydrogen cycles following sulfur deposition (indicated with arrows), the gate voltage shift between the hydrogen and oxygen pulses is reduced by a factor of ~ 3 compared to the response to similar pulses on the clean surface, demonstrating that sulfur contamination

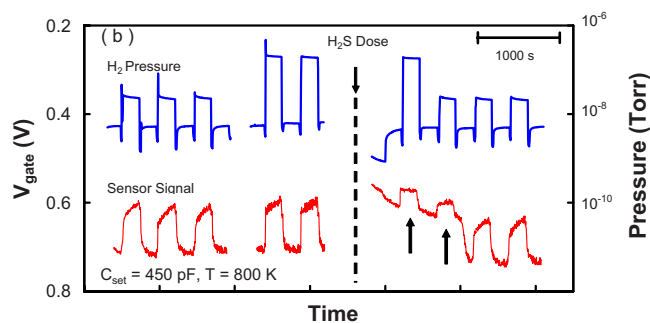


FIG. 8. (Color online) Sensor response to a sequence of alternating hydrogen and oxygen pulses, starting from a clean sample, before and after exposure to a pulse of hydrogen sulfide. An AES spectrum immediately after the H_2S dose showed a sulfur coverage of 0.4 ML. For the first two hydrogen pulses after the H_2S dose (indicated with arrows), the sensor's voltage shift is reduced by $\sim 70\%$ compared to the clean gate. After the third pulse, the sensor returned to its clean-gate behavior. An AES spectrum at the end of the sequence found no detectable sulfur on the surface. From Kahng, Tobin, Loloee, and Ghosh, J. Appl. Phys. **102**, 064505 (2007). ©2007, American Institute of Physics.

adversely affects device response. The primary reason for this reduced response is that the first two oxygen pulses do not bring the bias back to its baseline level, suggesting that adsorbed sulfur interferes with the surface reactions by which oxygen removes hydrogen, possibly by impeding the dissociation of oxygen molecules.

The third oxygen pulse restores the device to its baseline condition, and subsequent sensor responses are comparable to those observed before the sulfur was deposited. An AES spectrum measured after the complete measurement sequence showed no detectable sulfur on the surface, and the C-V curve of the device was unchanged from before the experiment. Exposure to oxygen, even at these very low pressures, effectively cleans the surface of adsorbed sulfur within a few minutes of exposure, probably by the formation and thermal desorption of sulfur dioxide (SO_2).

The kinetics of the sulfur removal reaction, however, are complex and depend strongly on the sulfur coverage. At high sulfur coverage, very few surface sites are available for oxygen dissociation and adsorption, and the reaction rate is extremely low. When enough sulfur has been removed that openings begin to appear in the sulfur layer, the reaction rate accelerates dramatically. This highly nonlinear behavior, which has also been reported in single-crystal studies,^{56–58} explains the abrupt reappearance of the sensor response after two hydrogen/oxygen cycles following sulfur exposure in Fig. 8. This behavior is explored and discussed in greater detail in Ref. 27. Even when the gate surface is saturated with sulfur, however (coverage of 0.6 ML), the sulfur can be completely removed by exposure to 10^{-4} Torr of oxygen for several minutes.²⁷

IV. CONCLUSION

The experiments presented above illustrate the crucial but indirect influence of oxygen on the functioning of SiC field-effect sensors with nonporous platinum gates. The sensor response arises from hydrogen atoms that diffuse from the gate surface to the metal/oxide interface. Catalytic oxidation of hydrogen to OH and to H_2O , followed by water

desorption, effectively removes hydrogen from the surface, reducing the hydrogen concentration at the metal-oxide interface sites. On a single device operated at low temperature and with a nonactivated gate, this reaction was found to be necessary for the complete depletion of the interface sites and therefore essential to the reversible operation of the sensor. For the higher catalytic activity and operating temperatures typical of operational devices, thermal desorption of hydrogen may be rapid enough for full reversibility, but these data nevertheless provide a clear illustration of the coupling between surface hydrogen-oxygen reactions and the occupation of metal/oxide interface sites. The oxidation reaction can also compete with the sensing process, reducing sensor response when the hydrogen/oxygen ratio is low. Finally, oxygen can also be important for removing undesirable impurities such as sulfur and carbon from the surface.

ACKNOWLEDGMENTS

This report was prepared with the support of the U.S. Department of Energy under Award No. DE-FC26-03NT41847. We thank Peter Tobias, currently at Honeywell, for his assistance and advice and V. H. S. Moorthy for preliminary experiments. The gate oxidation was performed by John Williams, Department of Physics, Auburn University.

- ¹N. G. Wright and A. G. Horsfall, *J. Phys. D* **40**, 6345 (2007).
- ²A. Lloyd Spetz, P. Tobias, A. Baranzahi, P. Mårtensson, and I. Lundström, *IEEE Trans. Electron Devices* **46**, 561 (1999).
- ³A. Baranzahi, A. Lloyd Spetz, B. Andersson, and I. Lundström, *Sens. Actuators B* **26**, 165 (1995).
- ⁴A. Lloyd Spetz, A. Baranzahi, P. Tobias, and I. Lundström, *Phys. Status Solidi A* **162**, 493 (1997).
- ⁵G. Müller, G. Krötz, and J. Schalk, *Phys. Status Solidi A* **185**, 1 (2001).
- ⁶A. Lloyd Spetz, L. Unéus, H. Svenningstorp, H. Wingbrant, C. I. Harris, P. Salomonsson, P. Tengström, P. Mårtensson, P. Ljung, M. Mattsson, J. H. Visser, S. G. Ejakov, D. Kubinski, L.-G. Ekedahl, I. Lundström, and S. M. Savage, *Mater. Sci. Forum* **389–393**, 1415 (2002).
- ⁷H. Wingbrant, H. Svenningstorp, P. Salomonsson, P. Tengström, I. Lundström, and A. Lloyd Spetz, *Sens. Actuators B* **93**, 295 (2003).
- ⁸H. Svenningstorp, B. Widén, P. Salomonsson, L.-G. Ekedahl, I. Lundström, P. Tobias, and A. Lloyd Spetz, *Sens. Actuators B* **77**, 177 (2001).
- ⁹A. Lloyd Spetz, L. Unéus, H. Svenningstorp, P. Tobias, L.-G. Ekedahl, O. Larsson, S. Savage, C. Harris, P. Mårtensson, R. Wigere, P. Salomonsson, B. Häggendahl, P. Ljung, M. Mattsson, and I. Lundström, *Phys. Status Solidi A* **185**, 15 (2001).
- ¹⁰M. Andersson, P. Ljung, M. Mattson, M. Löfdahl, and A. Lloyd Spetz, *Top. Catal.* **30–31**, 365 (2004).
- ¹¹R. Loloee, B. Chorpening, S. Beer, and R. N. Ghosh, *Sens. Actuators B* **129**, 200 (2008).
- ¹²H. Wingbrant, H. Svenningstorp, P. Salomonsson, D. Kubinski, J. H. Visser, M. Löfdahl, and A. Lloyd Spetz, *IEEE Sens. J.* **5**, 1099 (2005).
- ¹³I. Lundström, S. Shivaraman, C. Svensson, and L. Lundkvist, *Appl. Phys. Lett.* **26**, 55 (1975).
- ¹⁴K. I. Lundström, M. S. Shivaraman, and C. M. Svensson, *J. Appl. Phys.* **46**, 3876 (1975).
- ¹⁵I. Lundström, *Sens. Actuators* **1**, 403 (1981).
- ¹⁶H. M. Dannetun, L.-G. Petersson, D. Söderberg, and I. Lundström, *Appl. Surf. Sci.* **17**, 259 (1984).
- ¹⁷L.-G. Petersson, H. M. Dannetun, and I. Lundström, *Phys. Rev. Lett.* **52**, 1806 (1984).
- ¹⁸L.-G. Ekedahl, M. Eriksson, and I. Lundström, *Acc. Chem. Res.* **31**, 249 (1998).
- ¹⁹L.-G. Petersson, H. M. Dannetun, J. Fogelberg, and I. Lundström, *J. Appl. Phys.* **58**, 404 (1985).
- ²⁰P. Kreisl, A. Helwig, G. Müller, E. Obermeier, and S. Sotier, *Sens. Actuators B* **106**, 442 (2005).
- ²¹P. Kreisl, A. Helwig, A. Friedberger, G. Müller, E. Obermeier, and S. Sotier, *Sens. Actuators B* **106**, 489 (2005).
- ²²A. Salomonsson, M. Eriksson, and H. Dannetun, *J. Appl. Phys.* **98**, 014505 (2005).
- ²³S. Nakagomi, A. Lloyd Spetz, I. Lundström, and P. Tobias, *IEEE Sens. J.* **2**, 379 (2002).
- ²⁴J. Schmalwig, P. Kreisl, S. Ahlers, and G. Müller, *IEEE Sens. J.* **2**, 394 (2002).
- ²⁵H. Wingbrant and A. Lloyd Spetz, *Appl. Surf. Sci.* **252**, 7473 (2006).
- ²⁶P. Tobias, B. Golding, and R. N. Ghosh, *IEEE Sens. J.* **3**, 543 (2003).
- ²⁷Y. H. Kahng, R. G. Tobin, R. Loloee, and R. N. Ghosh, *J. Appl. Phys.* **102**, 064505 (2007).
- ²⁸H. Katsuta and R. B. McLellan, *J. Phys. Chem. Solids* **40**, 697 (1979).
- ²⁹A. E. Åbom, R. T. Haasch, N. Hellgen, N. Finnegan, L. Hultman, and M. Eriksson, *J. Appl. Phys.* **93**, 9760 (2003).
- ³⁰J. L. Gland, B. A. Sexton, and G. B. Fisher, *Surf. Sci.* **95**, 587 (1980).
- ³¹D. C. Skelton, R. G. Tobin, G. B. Fisher, D. K. Lambert, and C. L. DiMaggio, *J. Phys. Chem.* **104**, 548 (2000).
- ³²R. N. Ghosh and R. Loloee (unpublished).
- ³³S. Dhar, S. R. Wang, and J. R. Williams, *MRS Bull.* **30**, 288 (2005).
- ³⁴R. N. Ghosh and P. Tobias, *J. Electron. Mater.* **34**, 345 (2005).
- ³⁵R. N. Ghosh and R. Loloee, 12th International Meeting on Chemical Sensors, July 2008, Paper No. MMA6.
- ³⁶A. Samman, S. Gebremariam, L. Rimai, X. Zhang, J. Hangan, and G. W. Auner, *Sens. Actuators B* **63**, 91 (2000).
- ³⁷M. H. Weng, R. Mahapatra, N. G. Wright, and A. B. Horsfall, *Meas. Sci. Technol.* **19**, 024002 (2008).
- ³⁸A. D. Brailsford, M. Yussouff, E. M. Logothetis, and M. Shane, *Sens. Actuators B* **25**, 362 (1995).
- ³⁹A. Baranzahi, P. Tobias, A. Lloyd Spetz, P. Mårtensson, L.-G. Ekedahl, and I. Lundström, *J. Electrochem. Soc.* **145**, 3401 (1998).
- ⁴⁰A. Baranzahi, A. Lloyd Spetz, M. Glavmo, C. Carlsson, J. Nytomt, P. Salomonsson, E. Jobson, B. Häggendahl, P. Mårtensson, and I. Lundström, *Sens. Actuators B* **43**, 52 (1997).
- ⁴¹S. Nakagomi, P. Tobias, A. Baranzahi, I. Lundström, P. Mårtensson, and A. Lloyd Spetz, *Sens. Actuators B* **45**, 183 (1997).
- ⁴²V. P. Zhdanov and B. Kasemo, *Surf. Sci. Rep.* **20**, 113 (1994).
- ⁴³J. L. Gland, *Surf. Sci.* **93**, 487 (1980).
- ⁴⁴A.-P. Elg, F. Esiert, and A. Rosén, *Surf. Sci.* **382**, 57 (1997).
- ⁴⁵K. Christmann and G. Ertl, *Surf. Sci.* **60**, 365 (1976).
- ⁴⁶M. Salmerón, R. J. Gale, and G. A. Somorjai, *J. Chem. Phys.* **70**, 2807 (1979).
- ⁴⁷K. Umezawa, T. Ito, M. Asada, S. Nakanishi, P. Ding, W. A. Lanford, and B. Hjörvarsson, *Surf. Sci.* **387**, 320 (1997).
- ⁴⁸J. L. Gland and V. N. Korchak, *Surf. Sci.* **75**, 733 (1978).
- ⁴⁹A. Winkler, X. Guo, H. R. Siddiqui, P. L. Hagans, and J. T. Yates, Jr., *Surf. Sci.* **201**, 419 (1988).
- ⁵⁰H. Wang, R. G. Tobin, D. K. Lambert, C. L. DiMaggio, and G. B. Fisher, *Surf. Sci.* **372**, 267 (1997).
- ⁵¹C. H. Bartholomew, P. K. Agrawal, and J. R. Katzer, *Adv. Catal.* **31**, 135 (1982).
- ⁵²T. E. Fischer and S. R. Kelemen, *J. Catal.* **53**, 24 (1978).
- ⁵³N. Barbouth and M. Salame, *J. Catal.* **104**, 240 (1987).
- ⁵⁴J. A. Rodriguez and J. Hrbek, *Acc. Chem. Res.* **32**, 719 (1999).
- ⁵⁵A. K. Neyestanaki, F. Klingstedt, T. Salmi, and D. Y. Murzin, *Fuel* **83**, 395 (2004).
- ⁵⁶H. P. Bonzel and R. Ku, *J. Chem. Phys.* **59**, 1641 (1973).
- ⁵⁷U. Köhler, M. Alavi, and H.-W. Wassmuth, *Surf. Sci.* **136**, 243 (1984).
- ⁵⁸S. Astegger and E. Bechtold, *Surf. Sci.* **122**, 491 (1982).